Effect of mould expansion on pattern allowances in sand casting of steel

F. Peters[1], R. Voigt[2], S. Z. Ou[3] and C. Beckermann*[3]

For steel castings produced in sand moulds, the expansion of the sand and have a significant impact on the final size and shape of the casting. Experiments are conducted using a cylindrical casting to study this effect for different sands (silica and zircon) and different sand binder systems (phenolic urethane and sodium silicate). The type of sand has a significant effect on the final casting dimensions, in particular because the expansion of silica sand can be irreversible. The sand expansion effect is enhanced by the presence of sodium silicate binder. In addition, the size of the core, which in the present experiments controls the amount of steel in the mould and thus the heat input to the mould, strongly affects the internal and external dimensions of the resulting casting. A combined casting and stress simulation code is used to predict the dimensional changes of the castings. In several cases, the pattern allowances are predicted successfully both for free and hindered shrinkage cases. Disagreements between the simulation results and the measurements can be attributed to the fact that the stress model does not account for the irreversible nature of the silica sand expansion, which is important when silica sand is heated to temperatures above $\sim$1200°C; and the outer mould sand surrounding the casting, which can cause inaccuracies when there is significant early mould expansion, hindrance, or movement.

Keywords: Steel casting, Pattern allowance, Sand expansion, Dimensional control, Casting simulation, Stress analysis

Introduction

Dimensional errors of castings can be divided into those due to random causes and those due to pattern errors. Random errors are the cumulative result of the many intermediate steps to produce a casting, such as core making, mould making, assembly of cores into the mould, mould closing, pouring, heat treating, cleaning and grinding. Random errors increase the variability of casting dimensions.

Pattern errors occur when the mean of the resultant casting feature is different from the specified feature size. When a new pattern is being designed, the dimensional changes of the mould and casting are estimated. These estimated changes are then applied to the pattern as what is traditionally called the shrinkage allowance or the shrink rule. This factor is referred to as pattern allowance (PA) in this paper, to reflect that there are more factors than shrinkage to be accounted for. The PA is defined as

$$\mathrm{PA}[\%] = \frac{\text{pattern feature size} - \textit{c}\text{asting feature size}}{\text{casting feature size}} \times 100 \qquad (1)$$

[1]Industrial and Manufacturing Systems Engineering Department, 2019 Black Engineering Bldg. Iowa State University, Ames, IA 50011, USA
[2]Industrial and Manufacturing Engineering Department, 0310 Leonhard Building, The Pennsylvania State University, University Park, PA 16802, USA
[3]Department of Mechanical and Industrial Engineering, 2402 Seamans Center, The University of Iowa, Iowa City, IA 52242, USA

*Corresponding author, email becker@engineering.uiowa.edu

There are many highly interdependent physical processes responsible for steel castings not having the same dimensions as the pattern from which the moulds are made. Shrinkage of the steel upon solidification and cooling to room temperature is the primary reason for dimensional changes. However, the mould also has the potential to change size, both before and after the metal is poured. The mould may also restrict the contraction of the metal during solidification.

When metal shrinkage is free or unrestrained by the mould and an air gap forms between the casting and the mould, the needed pattern allowance can readily be predicted as discussed below. However, portions of a casting can contract onto a core or certain parts of the mould. In these cases, stresses develop and the resulting casting contraction depends on the mechanical and physical properties of the sand and the solidifying steel. Such hindered shrinkage of restrained casting features is usually less in magnitude than free shrinkage. Stresses also develop due to non-uniform cooling of the casting which can result in casting distortion.

The final dimensions of a steel casting are also strongly influenced by volumetric changes of the mould and core sands. The high pouring temperature of steel can cause significant early heating and thermal expansion of the mould sand. When the metal is mostly liquid it offers little resistance and the sand can expand into the cavity. This expansion is arrested when metal develops a solidified shell against the sand. Since the sand aggregate is a good insulator, the zone of heat affected mould

Received 14 November 2006; accepted 5 November 2007
DOI 10.1179/136404607X268247

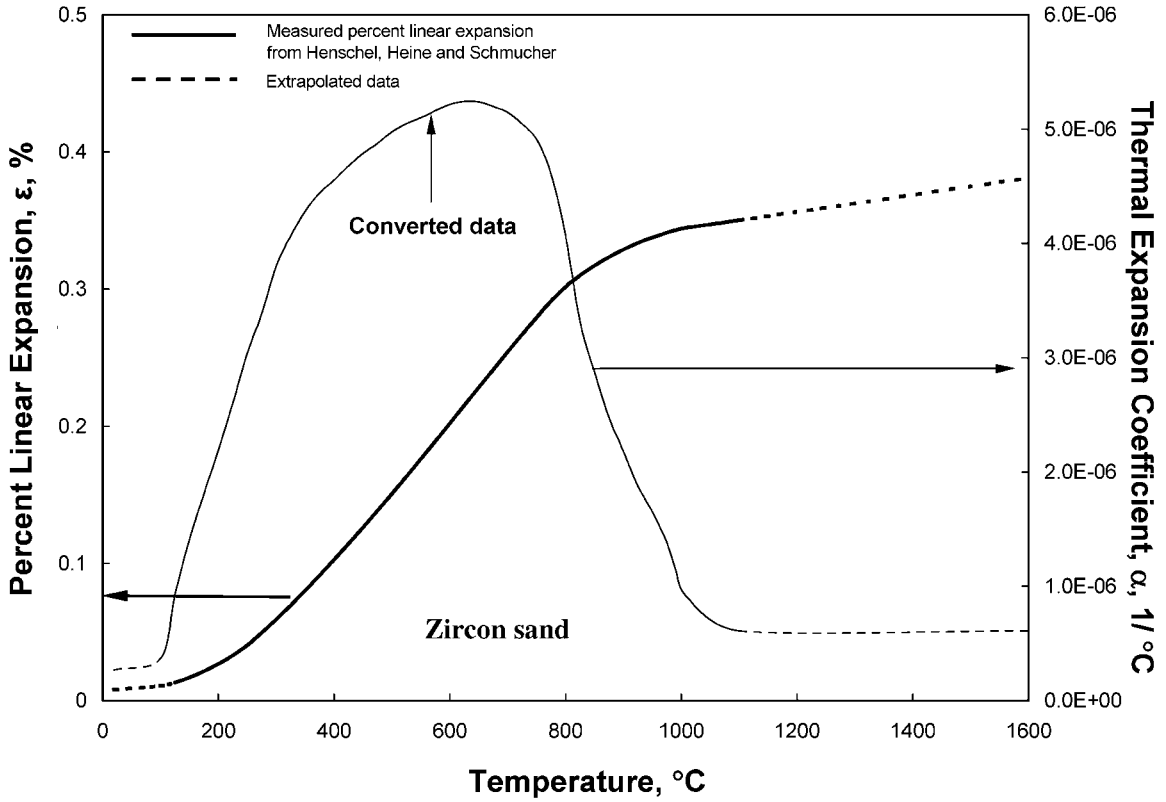

1 Percentage linear expansion and thermal expansion coefficient of zircon sand as function of temperature

material is typically narrow. The magnitude of sand expansion depends on the type of sand, as well as the binder system used.

Zircon sand is the common name for zirconium silicate ($ZrSiO_4$). Zircon sand has only one phase within the temperature range encountered in metal casting. The expansion of zircon is linearly dependent on temperature up to 1000°C; from room temperature to 1000°C, zircon expands by 0·3%.[1] Beyond 1000°C, the expansion levels off. Figure 1 shows the expansion curve for zircon sand based on data from Henschel *et al.*[2] Since the expansion characteristics of zircon sand are expected to be very predictable, zircon cores can provide critical information on the restraint offered by the sand to the contracting steel.

Unlike zircon sand, silica sand can undergo phase transformations with associated dimensional changes in the temperature range seen in steel casting applications. Therefore, a brief discussion of silica phases and transformations is provided to understand the experimental results. There are 22 known phases of silica. However, this discussion will be limited to low and high quartz, tridymite, and low and high cristobalite. The transformation from one phase to another is dependent on the temperature, time at temperature, and the presence of other substances.[3] The equilibrium inversion point for low quartz to high quartz is 573°C. This inversion is accompanied by an expansion, reported to be in the range of 1·1 to 1·6%. Sources agree that the inversion will rapidly occur if the inversion temperature is attained. Upon cooling, the inversion back to low quartz can also be rapid.[1,3–5] The theoretical inversion temperature of quartz to tridymite is 870°C. Sosman[3] reported that the conversion of quartz to cristobalite is favoured over conversion to tridymite. Cristobalite is the stable phase of silica above 1470°C. Quartz can convert directly to cristobalite at temperatures as low as 870°C. Sosman reports that the speed of the formation of cristobalite is slow below 1200°C, but becomes rapid above 1300°C. The reaction is strongly influenced by the presence and amount of other substances.[3] There is evidence that these sand transformations occur rapid enough to affect the mould and casting. For instance, common sand casting problems such as spalling, buckling and scabs are the result of sand expansion due to transformations.[1] Carniglia[5] noted that it is impossible to convert cristobalite or tridymite back to quartz above 870°C, because the latter phase is not stable at such high temperatures. At temperatures below 870°C, kinetic barriers are too high to allow this conversion to occur.[5]

Andrews *et al.*[6] measured the linear thermal expansion of sand moulding materials with different binders for various additions of iron oxide, and under a simulated mould atmosphere. The results for silica sand show a large linear expansion of up to 12% at temperatures above 1200°C. This expansion is attributed to the formation of cristobalite.[3,7] These results are shown in Figs. 2 and 3.

A search of the literature did not reveal any methods to predict the shrinkage of features on complex metal castings a priori. However, several bodies of research provide insight into the subject. Bates and Wallace[8] measured the mould wall displacement with an implanted probe in green sand and sodium silicate bonded moulds used to produce steel castings. For sodium silicate bonded moulds, the mould wall expansion was limited by the high strength of the bond and the absence of a weak high moisture layer found in green sand moulds. Mould displacements occurred before a

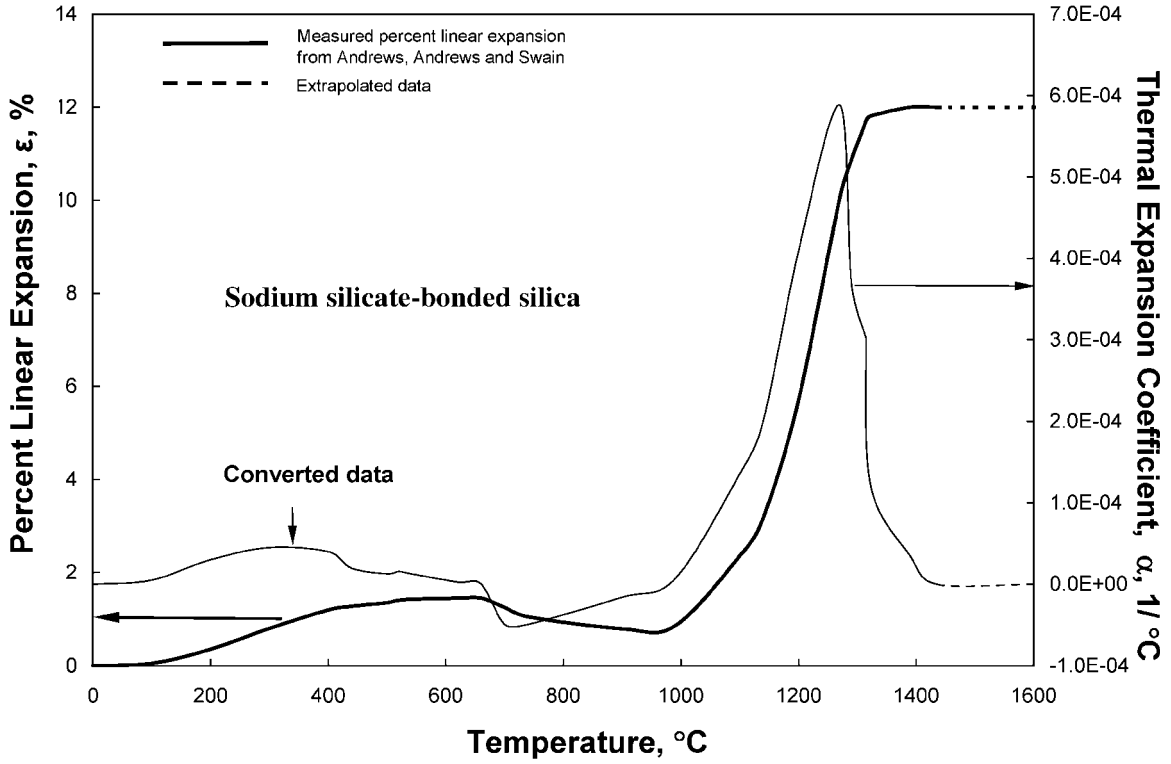

2 Percentage linear expansion and thermal expansion coefficient of sodium silicate bonded silica sand as function of temperature

sufficient skin of solidified steel was formed. Engler *et al.*[9] showed that green sand moulds, which were heated via radiation, exhibited mould wall displacements similar to moulds in which steel was poured, indicating that the hydrostatic pressure from the liquid steel was not an important variable. Mould wall displacement for green sand and chemically bonded sand moulds was measured with linear transducers by Rickards.[10] Ward[11] separated mould displacements that occur during casting into permanent linear changes and mould dilation. The permanent linear change of the mould was defined as the irreversible dimensional

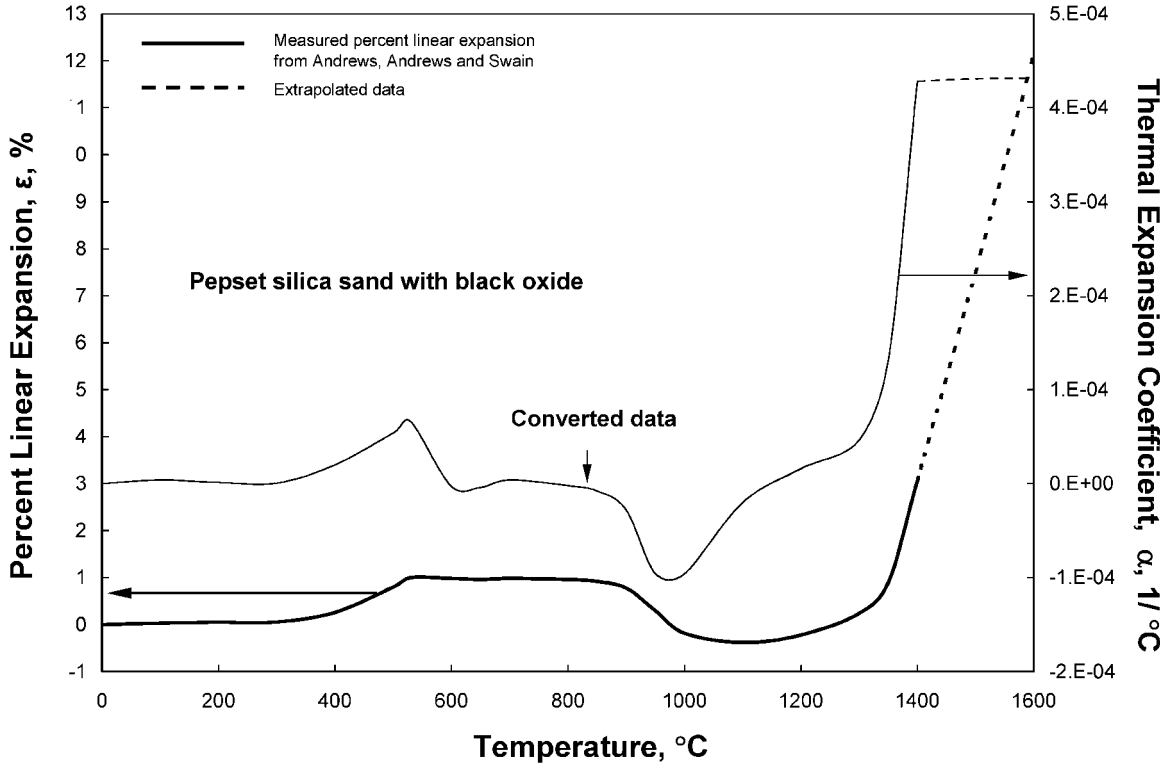

3 Percentage linear expansion and thermal expansion coefficient of phenolic urethane bonded sand (with black oxide addition), as function of temperature

changes of the mould after being heated and cooled. Ward concluded that the binder systems that exhibited the greater permanent linear change (presumably sand expansion) had the smallest mould displacement caused by the metal. Henschel *et al.*[2] investigated the effect of mould dilation on the pattern allowance. They measured the linear expansion properties of silica, zircon and olivine sands up to 1093°C during solidification of white iron, nodular iron, Al–Si alloys and Ni–Al bronze. Their results show that mould/core expansion and lack of strength or density in parts of the mould play an essential role in determining the pattern allowance. Several studies have used statistical methods to formulate relationships between the pattern allowance and factors, such as the casting method, degree of hindrance, or presence of parting line.[12–15] Aubrey *et al.*[14] demonstrated the difficulty of determining the pattern allowance for steel castings, particularly for dimensions less than 25·4 mm.

Briggs and Gezelius[16] measured the shrinkage of 0·35%C steel under various restraints. They found that the pattern allowance for free shrinkage is equal to 2·4%, and for hindered shrinkage the pattern allowance ranges from 0·39 to 2·4%. They noted that the outer skin of the casting never exceeded 1400°C, which indicated the immediate solidification of a thin outer shell on the casting. Moore[17] indicated that thick sections undergo less contraction, because molten metal can feed these areas and compensate for a portion of the contraction.

Many foundries are using computer simulation to design castings, however, to date, casting simulation is rarely used by industry to predict pattern allowances. Computer simulation of mould filling and solidification has attained a relatively high level of maturity, and gating and riser design can reliably be done using simulation. Casting simulation software has become available that allows for the calculation of stresses and strains during casting due to thermal effects and volume changes. This capability may allow for the prediction of the dimensional changes occurring during solidification and cooling and, thus, of pattern allowances.

An excellent overview of available software for the thermomechanical analysis of castings can be found in the recent study by Kron *et al.*[18] This study compared the abilty of different software packages in predicting the air gap formation in casting of aluminium alloys in a steel mould. A poor knowledge of the mechanical constitutive equations needed in thermomechanical casting simulations was pointed out. In addition, it was noted that the treatment of the contribution of the solidification shrinkage to the total strain in the solidifying metal is not yet satisfactory.

The primary objective of the present study is to investigate the effect of sand expansion on the pattern allowance in casting of steel. Experiments are performed for a simple cylindrical casting geometry with different core diameters and various sand and binder combinations. The experiments not only allow for an increased understanding of the effect of sand expansion on pattern allowances, but also provide benchmark data for comparison with predictions from computer simulations. Thus, a second objective of the present study is to use the experimental data to assess the ability of a common simulation code (The code MAGMASOFT is used in the present study. The use of MAGMASOFT is in no way intended to endorse this particular software) to predict pattern allowances in steel casting. The present experiments provide a stringent test of such simulations, because the measured pattern allowances are strongly affected by both sand expansion and constrained contraction, such that large stresses can develop. To the authors' best knowledge, a detailed comparison between pattern allowances obtained from casting simulation and from carefully controlled experiments has not been reported in the open literature.

The experimental procedures and the results of the casting experiments are presented next. This is followed by a discussion of the computer simulation methods and results including any disagreements between the measured and predicted pattern allowances.

Experimental procedures and results

Test castings were produced to study the influence of moulding materials, mould binder, and core size on the resultant steel casting size. The cylindrical test casting was 203·2 mm in length and 101·6 mm in outside diameter. The cylindrical cores of two diameters (either 76 or 25 mm) ran the entire length of the casting. The patterns and coreboxes were machined from wrought 6061 aluminium. The castings were produced two per mould; the castings were horizontal and parallel to each other as shown in Fig. 4. A single riser, placed on one end of the casting, was utilised to feed both castings. The single riser allowed the other end of the cylinders to contract upon solidification. An exothermic sleeve was utilised around the riser to minimise its size. The metal was poured directly into the riser, eliminating the need for a gating system which would have caused restraint during solidification. The objective of the casting design was to be able to study features that are affected by sand behaviour. There will be dimensional variations along the length of the casting, but this experiment specifically investigated external and internal diameters near the centreline of the casting, which is an area out of the immediate influence of the riser.

The moulds and cores were produced using two different binders, an organic phenolic urethane binder (Pepset) and Accoset brand inorganic ester cured sodium silicate binder (SodSil), both from Ashland Chemical. The moulds and the silica sand cores were made from washed 70 AFS grain fineness Wedron silica sand. DuPont brand zircon sand was used to produce the remaining cores. For the phenolic urethane, 1·3 and 0·6% binder by weight was used when mixed with silica and zircon sand respectively. Similarly, 3·9 and 2·1% of the sodium silicate binder was used. These binder levels were typical of that used in production foundries. Iron oxide was added to the sand when the phenolic urethane binder was used to prevent veining, as is common practice. All of the moulds and cores were produced on a Palmer continuous sand mixer. For mould production, the mixed sand was discharged directly into the flask, and lightly compacted. When making the cores, the sand was mixed and then scooped into the slender corebox, and manually rammed. To insure core to core consistency for the trials, only cores with consistent weights were used. For each of the eight core combinations, the percentage difference between the heaviest and lightest core was less than 3·1%. A 2^4 full factorial (mould binder, core sand, core binder, core size) experimental

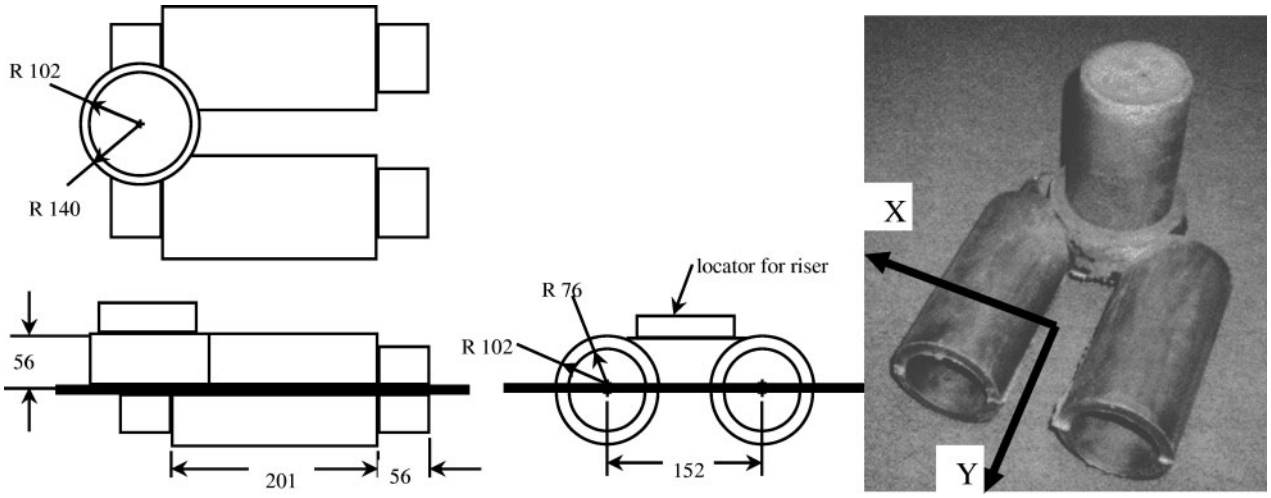

4 Drawing of pattern used to make moulds, and photograph of test casting with coordinate system used in simulation defined (all units in mm)

design trial with two replicates was conducted, requiring 32 castings to be poured. The placement of cores within the moulds and the pouring order were randomised.

Four diameter measurements were made on each mould, core and casting feature. Each measurement was on the half diameter, 12·7 mm from the each side of the centreline. To capture all of the dimensional changes that occurred at that location on the cylinder, but excluding the effect of the parting line, each half diameter was calculated from eight equally spaced points. All measurements were made on a Brown and Sharpe *Microval* CMM. To access the internal casting diameter, the castings were cut in half perpendicular to the axis of the cylinder.

Instead of using the corebox or pattern dimensions, the actual size of the moulds and cores were used to determine the amount of shrinkage to eliminate the inclusion of moulding variability. All of the experimental results presented were calculated by substituting the core or mould size for 'Pattern feature size' in equation (1).

Dimensional measurements of the moulds, cores and castings could have significant measurement error for several reasons. The direct surface measurements of the moulds and cores could be inconsistent due to loosening sand grains. Measurement errors were also likely introduced by manually locating the probe and selecting the measurement points. To overcome these measurement problems, each feature measurement was repeated at least twice. If the difference between the measurements was greater than 0·025 mm, the measurement was repeated until the difference between two measurements was less than this criterion. For all subsequent calculations, the average of the two measurements was used.

The moulds were transported to a commercial steel foundry for pouring. A sodium silicate mould paste was used to bond the mould halves. All of the moulds were poured from a single induction melted heat of WCB grade low carbon steel. The pouring temperature was maintained between 1600 and 1620°C. The castings were allowed to cool to room temperature before shakeout. The castings were then lightly shot blasted in a tumble blaster just long enough to clean the exterior surface. The risers were removed with an abrasive cut-off saw. The internal casting surfaces were also gently blasted after they were sawed in half. The castings were measured in the as cast condition. A representative casting with the 25 mm internal diameter was gamma ray inspected, which revealed acceptable class 2 shrinkage porosity.

The experiment was originally designed such that there would be two castings for each combination of independent variables. Due to experimental problems, a second replicate was not complete but a single replicate was successfully attained.

Table 1 presents the individual PA values for the external diameter of the castings, which is formed entirely by the mould. In all cases, the moulds were made of silica sand, bonded with one of the two binder systems. While the core sand and binder is reported in the table, it is not expected to have an influence on the external casting geometry. This expectation holds true. The dimensional change which would be caused solely from steel shrinkage is 2·4%, as reported by Briggs and Gezelius.[16] The measured shrinkage values ranged from 2·0 to 3·9%, with an average of 2·8%. When separated by the core size, the average shrinkage values for the castings with the 25 and 76 mm cores were 3·3 and 2·3% respectively. This difference can be explained by the fact that the castings with the 25 mm cores contained more steel to heat the sand and subsequently causing the sand mould surfaces to expand. In addition, the solidification of the steel for these castings took a longer time, so there was more time in which the sand could expand before its movement was resisted by solidifying steel that had gained sufficient strength.

To represent the most common industrial practice, the castings were produced horizontally in the mould. The cope and drag halves of the moulds and castings were measured and used to independently determine the dimensional changes for each side of the parting. There was not a significant difference between the dimensional changes of the cope and drag locations, for either the external or internal features. Therefore, all four measurements for each casting feature (cope and drag, on each side of the centerline) were averaged and this is the data presented here.

The measured pattern allowance values for the internal diameters of the castings, which are formed entirely by the core, are shown in Table 2. The

Table 1 Measured pattern allowances (PAs) for external casting diameter*

Mould binder	Core binder	Core size, mm	Core sand	PA of individual replications			Simulation case
Pepset	Pepset	25	Silica	3·5%	3·7%		
Pepset	Pepset	25	Zircon	3·9%	3·9%		
Pepset	SodSil	25	Silica	3·2%	3·8%	3·8%	Case 3
Pepset	SodSil	25	Zircon	3·9%	3·6%		
Pepset	Pepset	76	Silica	2·2%	2·3%		
Pepset	Pepset	76	Zircon	2·6%	2·4%	2·4%	Case 1
Pepset	SodSil	76	Silica	2·3%			Case 2
Pepset	SodSil	76	Zircon	2·4%			Case 1
SodSil	Pepset	25	Silica	2·1%	3·0%		
SodSil	Pepset	25	Zircon	3·2%			Case 4
SodSil	SodSil	25	Silica	2·4%			
SodSil	SodSil	25	Zircon	3·5%			Case 4
SodSil	Pepset	76	Silica	2·0%	2·2%		
SodSil	Pepset	76	Zircon	2·1%			
SodSil	SodSil	76	Silica	2·1%	2·1%	2·1%	
SodSil	SodSil	76	Zircon	2·5%	2·3%	2·4%	

*The external diameter of all castings was 102 mm. Cases used for the simulations are identified in the final column.

dimensions of the inside diameters varied significantly more than seen for the external diameters. The values ranged from a shrinkage of 2·9% to an expansion of 15·9% (reported as a negative shrinkage value in the table). As expected from the expansion properties of zircon sand, the dimensional changes of the internal diameters created by the zircon cores were very consistent regardless of core diameter. The pattern allowance values ranged from 1·3 to 2·9%, with an average of 1·5%. There were only two values above 1·6%, so these remain suspect because of the measurement challenges presented by measuring sand cores and rough casting surfaces. The sand cores will restrain the solidifying steel. Based on Briggs'[16] research on steel shrinkage that is restrained, the shrinkage of the internal features was expected to be less than the unrestrained steel shrinkage value, 2·4%. The internal diameters formed by the 76 mm cores made of silica sand had very consistent pattern allowance values, from 0·2 to 0·4%. The difference in shrinkage of these diameters compared to those made with zircon cores can be explained by the expansion behaviour of the silica sand. Before the steel solidified, the silica sand expanded, effectively increasing the diameter of the core. The internal diameters created by the 25 mm silica sand cores experienced the most dramatic dimensional changes. The internal casting diameters with silica sand bonded with phenolic urethane binder were on average 4·4% larger than the cores. This can only be explained by expansion of the sand before the steel developed a strong enough shell to resist the core expansion. The silica sand cores bonded with sodium silicate binder expanded even more, 15·3% on average. This difference can be explained by comparing the bonded sand expansion characteristics measured by Andrews *et al.*[6] and displayed in Figs. 2 and 3.

The smaller cores experienced higher temperatures for a longer duration, causing more expansion than for the larger cores. In addition to the expansion, the 25 mm cores made of silica sand and the sodium silicate binder underwent major shape changes before solidification. Visual observation indicated that the centre of these cores bowed upwards $\sim$25 mm.

Simulation procedures and results

The experimental data presented in Tables 1 and 2 are now used to assess the ability of a casting simulation code to predict the dimensional changes that occurred in the test castings. The simulations also allow for an increased insight into the thermomechanical phenomena that lead to the observed pattern allowances.

Simulation procedures

The simulations were performed using the casting simulation software MAGMASOFT, including the

Table 2 Measured pattern allowances (PAs) for internal casting diameter*

Mould binder	Core binder	Core size, mm	Core sand	PA of individual replications			Simulation case
Pepset	Pepset	25	Zircon	1·4%	1·0%		
SodSil	Pepset	25	Zircon	2·9%			Case 4
Pepset	SodSil	25	Zircon	2·1%	1·4%		
SodSil	SodSil	25	Zircon	1·3%			Case 4
Pepset	Pepset	76	Zircon	1·6%	1·3%	1·5%	Case 1
SodSil	Pepset	76	Zircon	1·3%			
Pepset	SodSil	76	Zircon	1·5%			Case 1
SodSil	SodSil	76	Zircon	1·4%	1·4%	1·4%	
Pepset	Pepset	25	Silica	−4·5%	−6·1%		
SodSil	Pepset	25	Silica	−3·6%	−3·2%		
Pepset	SodSil	25	Silica	−15·9%	−14·9%		Case 3
SodSil	SodSil	25	Silica	−15·2%			
Pepset	Pepset	76	Silica	0·4%	0·4%		
SodSil	Pepset	76	Silica	0·3%	0·4%		
Pepset	SodSil	76	Silica	0·4%			Case 2
SodSil	SodSil	76	Silica	0·4%	0·2%	0·3%	

MAGMAstress module.[19] A detailed description of this code can be found in Kron *et al.*[18] A thermal simulation is performed first and the calculated temperature distributions at various times during solidification and cooling are then input into the MAGMAstress module. Hence, the thermal and mechanical calculations are not directly coupled. The stress simulations use a thermo–elastic–plastic mechanical constitutive relation derived from the Prandtl-Reuss equations.[18]

The thermal expansion coefficients for the sands were obtained from the data in Figs. 1–3. Figures 1–3 are from experiments that measured the relative change of length, $\varepsilon = \Delta L/L$, rather than the thermal expansion coefficient α that is used in the simulation software. These two quantities are related by

$$\alpha = \frac{\varepsilon}{\Delta T} \tag{2}$$

where ΔT is the temperature interval over which the sand expands by a length ΔL. The conversion from the graphs of $\varepsilon(T)$ to $\alpha(T)$ was done numerically using the following formula

$$\alpha(T_i) = \frac{\varepsilon_i - \varepsilon_{i-1}}{(T_i - T_{i-1})(1+\varepsilon_{i-1})} \tag{3}$$

where ε_i (ε_{i-1}) is the relative change of length at temperature T_i (T_{i-1}) and the subscript i denotes a discrete point on the graph $\varepsilon(T)$. The interval between points i and $i-1$ was chosen sufficiently small so as to obtain an accurate, but smooth, conversion. The converted data for $\alpha(T)$ are also shown in Figs. 1–3 using the scale on the right hand side of the graphs. Some extrapolation of the data above the measured temperature range was necessary because the sand reaches temperatures as high as 1500°C. The accuracy of these extrapolations is not known, but they are believed to have a relatively minor effect on the present pattern allowance predictions.

The thermal expansion coefficient for WCB steel was obtained from the density data output by the interdendritic solidification software IDS developed by Miettinen.[20,21] The thermal expansion coefficient α in units of 1/°C, was obtained from the density ρ through the following relation

$$\alpha = -\frac{1}{3\rho}\frac{\partial \rho}{\partial T} \tag{4}$$

The other thermal properties of the WCB steel, as well as the solid fraction versus temperature relationship, were also generated using IDS and input into the MAGMASOFT database. All other properties needed in the simulations, including the mechanical properties needed for the MAGMAstress module, were taken from the MAGMASOFT database. Filling simulations were not performed, because the effect of filling on the temperature distribution is small for the heavy section castings simulated here. A constant and uniform interfacial heat transfer coefficient between the steel and the sand/core of 1000 W m^{-2} K^{-1} was used. In sand casting of steel, as opposed to permanent mould casting of aluminium alloys for example, the predicted temperatures are not very sensitive to this coefficient, because the steel and the sand itself represent the major thermal resistances. In unpublished work by two of the present authors (S.O. and C.B.), thermocouples were inserted into a variety of WCB steel sand castings and excellent agreement between measured and predicted temperatures was obtained using the same simulation parameters and properties as in the present study. Thus, the thermal part of the present simulations can be considered to be highly accurate.

A few other remarks are needed regarding the stress simulations. First, the irreversible nature of the silica sand expansion at high temperatures is not taken into account in the MAGMAstress module. In other words, the code assumes that during cooling, the thermal expansion coefficient follows the lines in Figs. 2 and 3. The effects of this simplification on the predictions are assessed below. Second, the outer mould sand surrounding the castings was excluded in the stress calculations (but not in the thermal simulations). This was done because MAGMAstress cannot account for the separation of the casting from the mould due to casting shrinkage and the formation of an air gap. If the outer mould parts were included, an unrealistic tension would be transmitted into the mould when an air gap forms. As discussed further below, the exclusion of the outer mould in the stress simulations can cause problems in cases where the mould/metal interface is in compression (e.g. due to sand expansion). The core was, however, taken into account in the stress simulations, because the core/metal interface is always in compression. Similarly, the sand between the two cylinders was included in the simulation as well. The riser and its removal was also simulated.

Four cases were selected to simulate the dimensional changes that occur in the castings (*see* Tables 1 and 2). The simulation results for each of these cases are described below, including discussion of discrepancies that were observed.

Free shrinkage: cylinder length

The first step in verifying the simulations is to examine the value of the pattern allowance predicted for the case of free or unrestrained shrinkage. An example of a feature that undergoes free shrinkage in the test castings is the length of the cylinder at the end opposite to the riser. Figure 4 provides the coordinate system used for the geometry definition. Figure 5 shows the Y direction (along the cylinder axis) displacements as a function of time at two points (S11 and S25) on the end of one of the cylinders for case 1 conditions in Table 3. The exact location of the two points is provided in Fig. 6. It can be seen from Fig. 5 that the points S11 and S25 both move in the negative Y direction, indicating shrinkage, with a total displacement equal to 2·44 and 2·71 mm in magnitude for S11 and S25 respectively. The reason S11 and S25 are not displaced by the same amount is that the cylinder solidifies and cools asymmetrically due to the presence of the shared end riser and of the other cylinder. Figure 6 shows the predicted 'zero displacement plane' (ZDP) for the Y direction displacements. The ZDP is somewhat skewed and shifted towards the riser end, instead of being exactly in the middle of the cylinder.

These results can now be used to calculate the pattern allowance for free shrinkage predicted by the simulation code. The pattern lengths from the ZDP to points S11 and S25 are 104·2 and 115·88 mm respectively (*see* Fig. 6). Using equation (1) and the displacement values noted above, the calculated pattern allowance is equal to

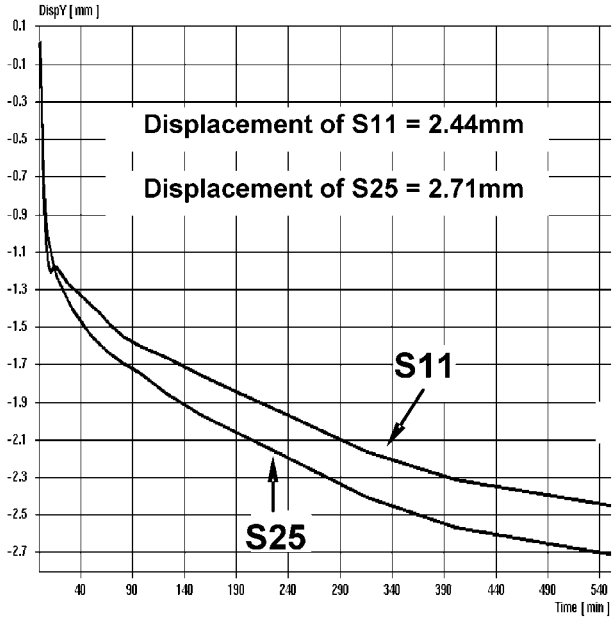

5 Predicted Y direction displacement at points S11 and S25 (*see* Fig. 6) as a function of time for case 1

2·4% for both points on the end of the cylinder. The pattern allowance for the cylinder length was not measured, so these values cannot be compared. However, the agreement of the predicted pattern allowance with the 2·4% pattern allowance value measured by Briggs and Gezelius[16] for free shrinkage establishes some confidence in the present simulations.

Hindered shrinkage in presence of reversible core expansion

The inner cylinder diameters for simulation cases 1 and 4 with a zircon core are examples of features that undergo hindered shrinkage in the presence of reversible core expansion. As the cylinder solidifies and cools, it contracts onto the core. The core is under compression, and the presence of the core provides a hindrance to the shrinkage of the casting inside diameter. Zircon expansion is linearly dependent on temperature up to 1000°C, where it reaches 0·3%, and then increases very little above that. The early expansion of the cores is not a result of a phase transformation, and therefore was considered reversible. Later contraction of the core upon cooling will also allow the surrounding steel to contract.

Before discussing the pattern allowance values, it is necessary to understand the differences in the

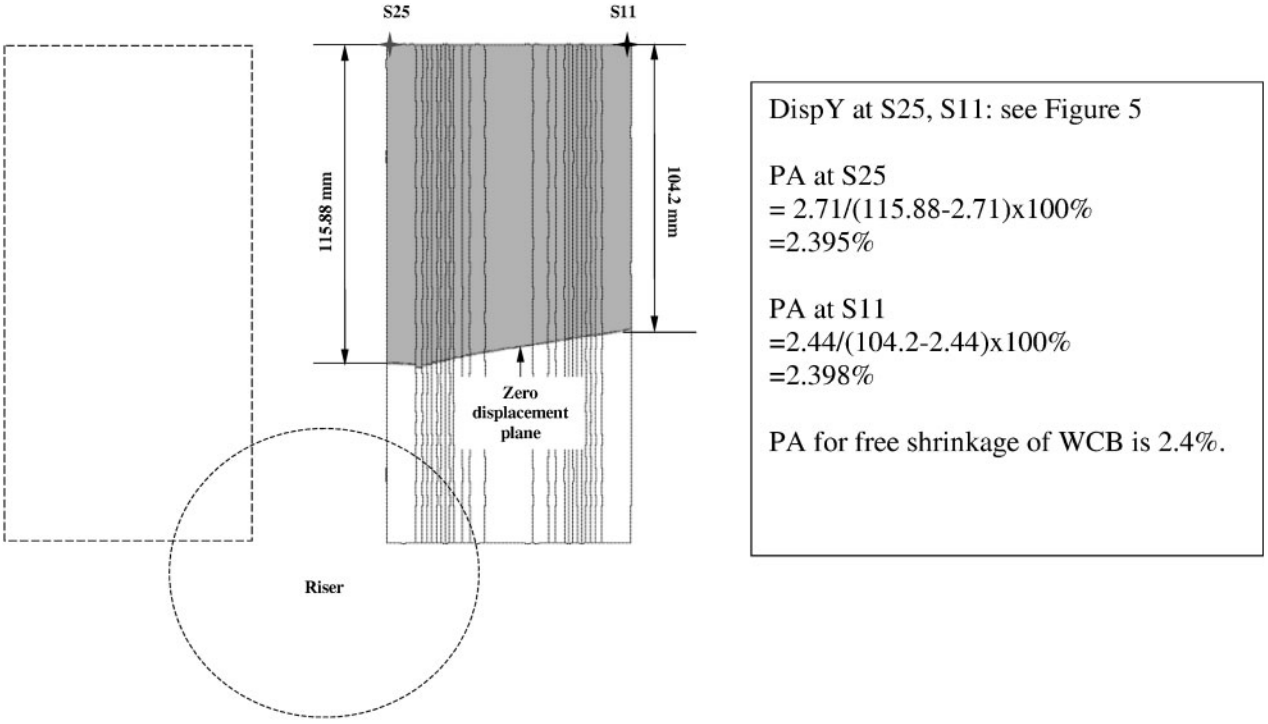

6 Illustration of calculation of free shrinkage at points S11 and S25 for case 1

Table 3 Measured and predicted pattern allowances (PA) for cylindrical test castings

Category		Case 1	Case 2	Case 3	Case 4
Mould		Binder: Pepset Sand: Silica	Binder: Pepset Sand: Silica	Binder: Pepset Sand: Silica	Binder: SodSil Sand: Silica
Core		Binder: Either Sand: Zircon	Binder: SodSil Sand: Silica	Binder: SodSil Sand: Silica	Binder: Either Sand: Zircon
Inner diameter (ID), mm		76	76	25	25
Outer diameter (OD), mm		102	102	102	102
PA–ID, %	Measured	1·3 to 1·6	0·4	−14·9 to −15·9	1·3 to 2·9
	Simulated	1·44	0·83	−2·84	1·64
PA–OD, %	Measured	2·4 to 2·6	2·3	3·2 to 3·8	3·2 to 3·5
	Simulated	1·79	1·54	1·98	2·18

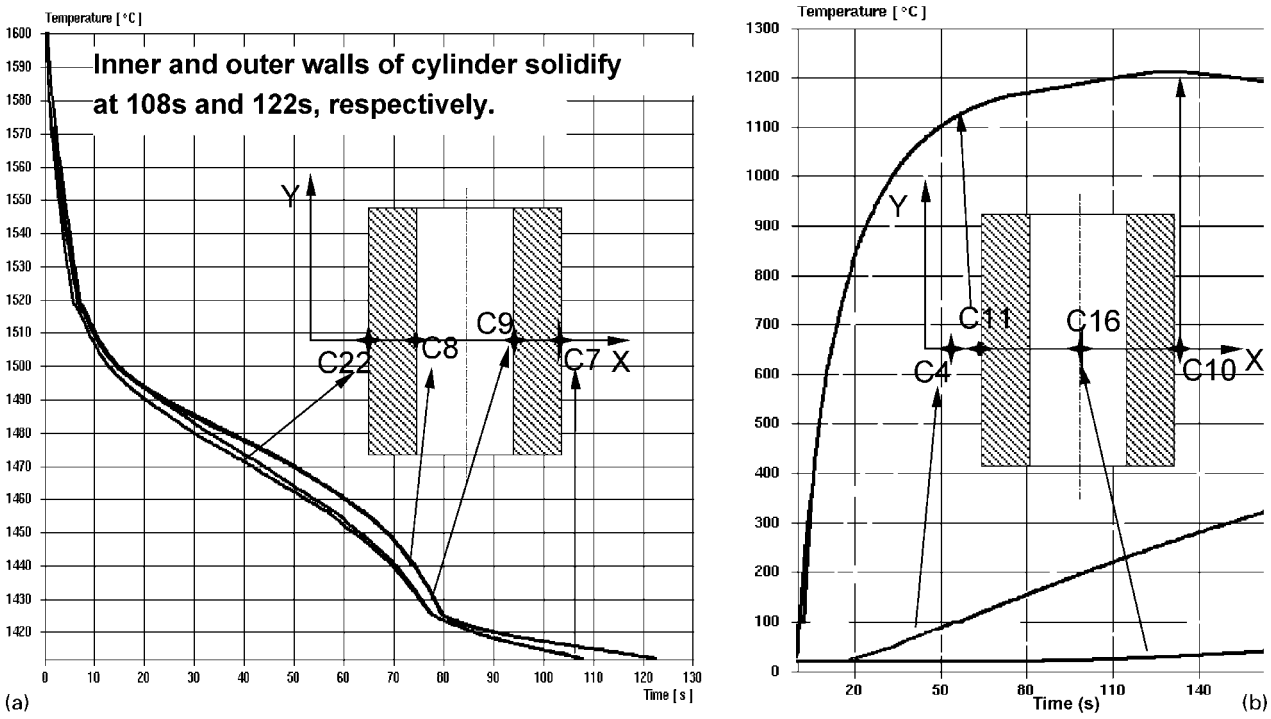

7 cooling curves *a* inside casting and *b* in mould/core for cases 1 and 2 (point C4 is 12·7 mm away from outer cylinder diameter, points C10 and C11 are in sand adjacent to outer cylinder diameter, while point C16 is in centre of core)

solidification and cooling behaviours for the cases with the large diameter cores (cases 1 and 2) and small diameter cores (cases 3 and 4). Figures 7–9 show cooling (temperature versus time) curves for various points of interest. For cases 1 and 2 with the 76 mm core, Fig. 7 indicates that the outer and inner walls of the cylinder solidify at 108 and 122 s respectively, after pouring. Furthermore, the sand adjacent to the outer (and inner) cylinder diameter heats up to $\sim$1200°C, and the sand at the centre of the core to less than 100°C. Hence, there are temperature differences of more than 1000°C inside the large diameter cores for cases 1 and 2. The temperatures are much different in cases 3 and 4 with the 25 mm core, because significantly more steel is present and the mass of the core is much less. Figure 8 shows that the inner and outer walls of the cylinder solidify at 16·4 and 12·1 min respectively, which is more than 10 min later than in cases 1 and 2. Sand temperatures for cases 3 and 4 are provided in Fig. 9. The small diameter core is almost isothermal and reaches a maximum temperature of 1500°C; this should be contrasted to the maximum temperature of less than 100°C at the centre of the large diameter core (cases 1 and 2). The sand adjacent to the outer diameter reaches $\sim$1300°C, which is also higher (by $\sim$100°C) than in cases 1 and 2. The sand 12·7 mm away from the cylinder still reaches a maximum temperature of almost 1200°C.

The predicted room temperature distortions, with the X direction displacements indicated by the grey scale, of the casting and the cores are shown in Figs. 10 and 11 respectively, for case 1. The X direction is the direction normal to the cylinder axis in the horizontal plane. Note that a relatively large magnification factor of 15 has been applied in order to make the distortions more visible in the figures. Figure 11 illustrates the deformation of the cores in case 1. It can be seen that the cylinders distort the cores. Figure 10 indicates that there is some distortion of the casting, with the non-riser ends of the two cylinders bending towards each other and the other ends held in place by the riser. Because of this uneven

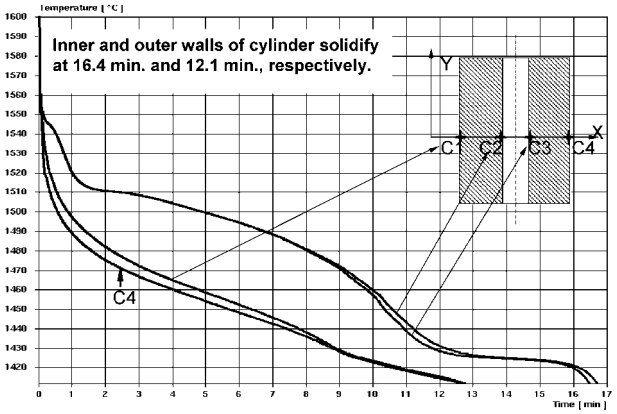

8 Predicted cooling curves inside casting for cases 3 and 4

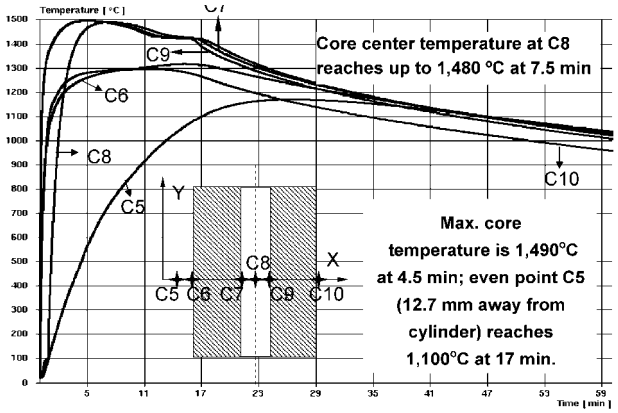

9 Predicted cooling curves in core and mould for cases 3 and 4

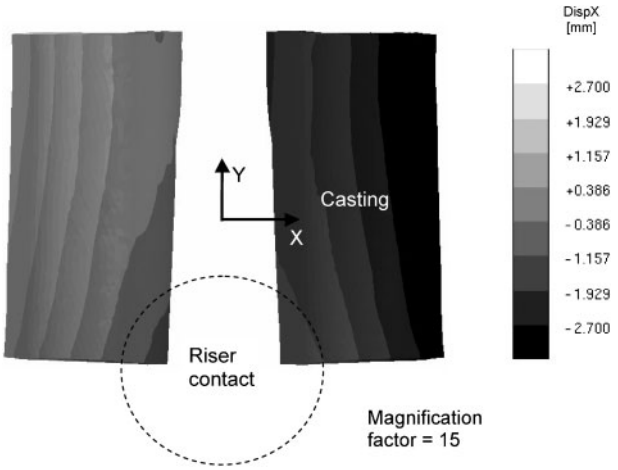

10 Predicted distortions (magnification factor of 15) of cast cylinders at room temperature in case 1; grey scale indicates X direction displacements on surface of cylinders

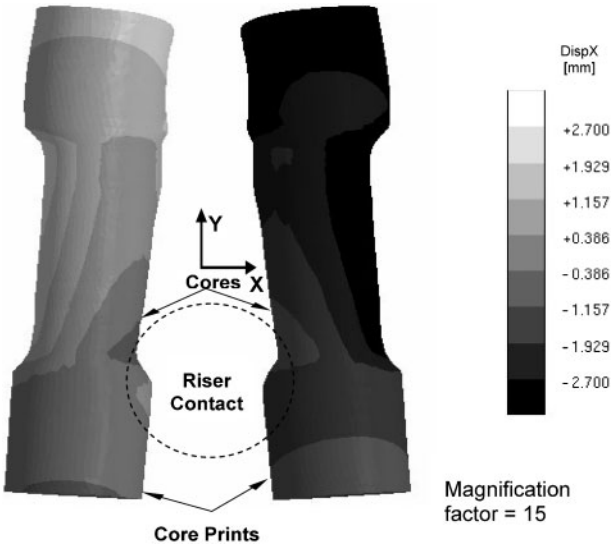

11 Predicted distortions (magnification factor of 15) of cores at room temperature in case 1; grey scale indicates X direction displacements on surface of cores

solidification and cooling, the displacement pattern on the surface of each cylinder is non-uniform. This non-uniformity, particularly at the ends of each cylinder, would result in different predicted pattern allowance values at each point on the cylinder. For the purpose of comparing to the measurements, only averages are reported here. The predicted pattern allowance values were averaged using between 14 and 22 points evenly distributed over the inner or outer cylinder surface. Although not shown here, the ranges in the predicted pattern allowance values are of a similar magnitude as the ranges in the measured pattern allowance values.

Returning now to the casting inner diameters for cases 1 and 4 with zircon cores, Table 3 shows that the predicted pattern allowance values are equal to 1·44 and 1·64% respectively. These predictions are in good agreements with the measurements, which range from 1·3 to 1·6% in case 1 and 1·3 to 2·9% in case 4. These pattern allowance values are considerably lower than the value of 2·4% for free shrinkage, because the shrinkage is hindered or restrained by the cores. The good agreement between the predictions and measurements indicate that the expansion of the zircon cores is indeed reversible and the mechanical behaviour of the materials in compression is modelled reasonably well. Note that there is a slight difference in the predicted pattern allowance values for the inner diameter between cases 1 and 4. This is caused by the different diameters of the cores, which result in different temperature distributions and expansion/contraction behaviours. Hence, pattern allowance values for restrained features are a function of the feature size itself.

Hindered shrinkage in presence of irreversible core expansion

Examples of hindered shrinkage in the presence of irreversible core expansion are provided by the inner cylinder diameter in cases 2 and 3. In these two cases the cores are made of sodium silicate bonded silica sand, as opposed to zircon sand in cases 1 and 4. The silica sand undergoes a much larger expansion at high temperatures than the zircon sand (*see* Fig. 1–3). The silica sand with either sodium silicate or phenolic urethane binder expands $\sim$1·2% when heated above 500°C, during the low quartz to high quartz phase transformation. If the sand/binder is heated above 1300°C, the silica sand will undergo a much greater expansion. The expansion is primarily caused by the transformation from quartz to cristobalite. This will cause a linear expansion of 12 and 5·5% for the silica sand bonded with the sodium silicate and phenolic urethane binders respectively. These values are based on the experimental values determined by Andrews *et al.*[6,22] The 1·2% expansion is reversible; however the larger expansion associated with the cristobalite transformation is considered irreversible. This irreversibility is not taken into account in the simulations, as noted earlier.

The predicted PA for the inner diameter in case 2 is 0·83% (*see* Table 3), which should be contrasted to the 1·44% PA predicted in case 1. The smaller PA for the inner diameter in case 2 compared to case 1 can be expected because of the larger core expansion in case 2. This effect is predicted even though the sand expansion is assumed to be reversible in the simulation. In case 3, the predicted pattern allowance for the inner diameter is −2·84%, which should be compared to 1·64% in case 4. The negative pattern allowance in case 3 indicates that the core is predicted to expand, which again can be attributed to the sand expansion properties of silica sand. The difference in the pattern allowance values between cases 3 and 4 is much larger than between cases 2 and 1, because of the difference in the core diameters (25 versus 76 mm). Since the smaller cores in cases 3 and 4 are heated to a much higher temperature (up to 1500°C, *see* Fig. 9), the core expansion will be much greater than for the larger cores in cases 1 and 2. In addition, the smaller cores were heated throughout, as opposed to the larger cores which only attained 100°C in the centre (*see* Fig. 7).

Table 3 shows that the quantitative agreement between the predicted and measured pattern allowances for the casting inner diameter in cases 2 and 3 is not good. The prediction that the pattern allowances in cases 2 and 3 are lower than in cases 1 and 4, and that the pattern allowance in case 3 is negative, is in qualitative agreement with the measurements. In both

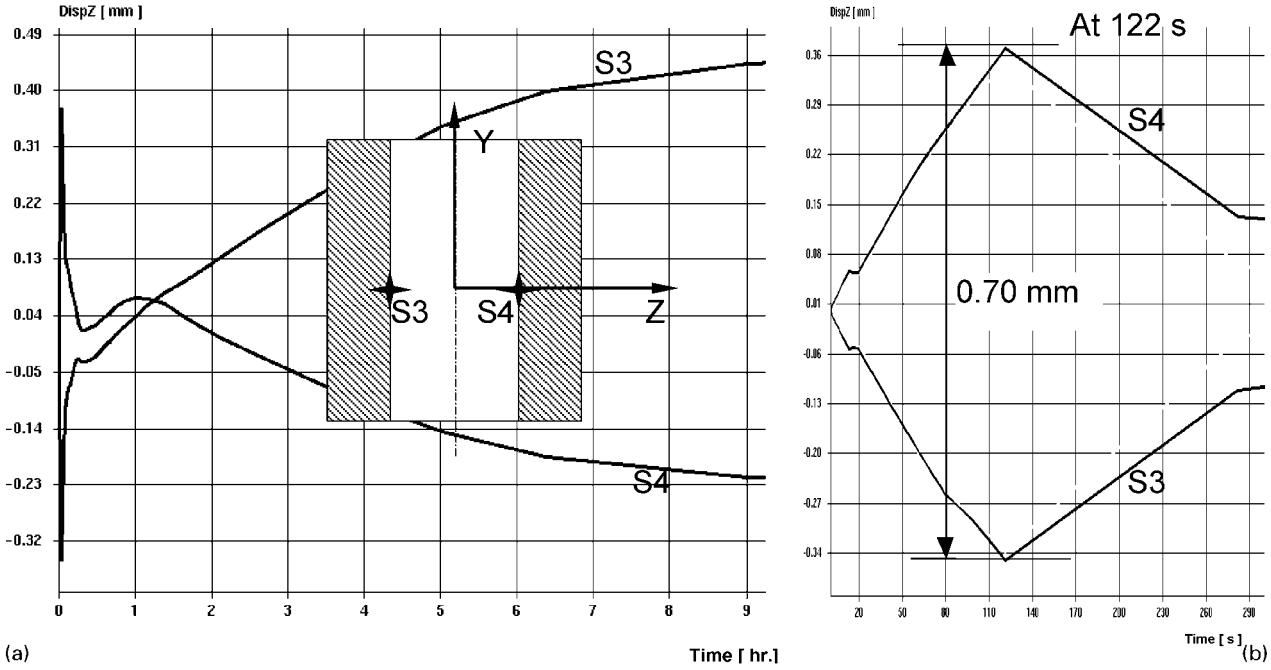

12 ***a*** **predicted Z direction displacements at points S3 and S4 in case 2 and** ***b*** **close-up of predicted displacements during first 290 s**

cases 2 and 3, however, the measured pattern allowances for the inner diameter are lower than the predicted pattern allowances. The difference is relatively small in case 2, but in case 3 it is large (less than −14·9% measured versus −2·84% predicted).

In order to verify that these differences are due to the fact that the simulation does not take into account the irreversibility in the core expansion, the magnitude of the effect of the irreversibility on the pattern allowance is estimated for cases 2 and 3. Figure 12 shows the predicted displacements of points S3 and S4 on opposite sides of the inside diameter as a function of time for case 2. It can be seen that before a solid steel shell forms at a time of 122 s, the inside (core) diameter is predicted to expand by 0·7 mm at this location (or 0·52 mm on average). Since in reality this expansion is irreversible, the core would not contract back upon cooling as rapidly as shown in Fig. 12. Thus, a rough estimate of the irreversibility effect can be obtained by subtracting the early (average) expansion of 0·52 mm from the predicted contraction in case 2 (0·63 mm) when calculating the pattern allowance. This is demonstrated in Table 4. The same procedure was applied in case 3. The pattern allowances corrected for irreversible sand expansion show much better agreement with the measured pattern allowances than those directly taken from the simulations. This indicates that irreversible core expansion is indeed responsible for the disagreement. The corrected pattern allowances in case 3 still underestimate the measured expansion, which may be attributed to the fact that the present correction procedure does not include the irreversibility effect after solidification begins. In particular, the irreversible expansion of the core would provide additional hindrance after solidification, which is not accounted for presently.

Partially hindered shrinkage in presence of irreversible mould expansion

The outer diameter (OD) of the cylinders can be considered a partially restrained feature because of the presence of the core on the inside of the cylinders. Partially restrained features can be expected to have pattern allowances less than that of unrestrained features that undergo free shrinkage (∼2·4%). However, Table 3 shows that the measured pattern allowance values for the partially restrained outer diameters are larger on the average, with the measured values being as high as 3·8%. Peters[23] attributed this effect to early expansion of the outer mould sand around the cylinders before a solid shell forms. The expanding mould would tend to push the outer cylinder diameter inwards, causing a reduction in the outer diameter, in addition to the one due to shrinkage of the steel. The size of the mould at the time a shell of solidified steel forms that can resist additional sand contraction can be defined as the 'effective mould size.' By estimating the

Table 4 Effect of irreversible core expansion on predicted pattern allowances (PAs) for inner cylinder diameter (ID) in cases 2 and 3, compared to measured values

	Shrinkage predicted before consideration of irreversible expansion of core sand		Predicted contribution of irreversible expansion of core sand		Shrinkage predicted with correction for irreversible expansion of core sand		Range of measured values
Case	Shrinkage, mm	PA–ID, %	Shrinkage, mm	PA–ID, %	Shrinkage, mm	PA–ID, %	PA–ID, %
2	0·63	0·83	−0·52	−0·68	0·11	0·15	0·4
3	−0·74	−2·84	−1·67	−6·57	−2·41	−9·41	−14·9 to −15·9

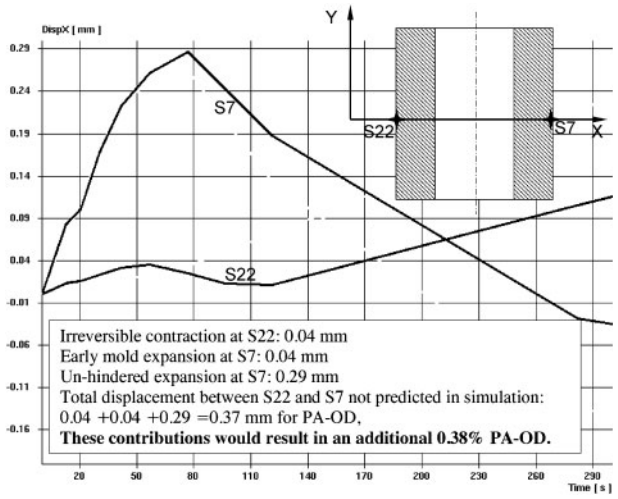

13 Predicted X direction displacements at points S7 and S22 in case 1

magnitude of this mould expansion effect, Peters[23] was able to predict the PA values for the partially restrained outer diameters and obtain good agreement with the measurements in all four cases of Table 3.

The simulations predict pattern allowance values for the outer diameter ranging from 1·54 to 2·18% in the four cases of Table 3. These pattern allowance values are lower than the one predicted for free shrinkage (2·4%) because of core hindrance. The pattern allowances for the outer diameter in cases 1 and 2 are predicted to be ~0·4% lower than in cases 3 and 4, because the larger core in cases 1 and 2 provides more hindrance. Furthermore, the predicted pattern allowances for the outer diameter in cases 2 and 3 with the silica sand core are ~0·2% lower than in the corresponding cases 1 and 4 respectively, with the zircon sand core.

Compared to the experimental measurements, where outer diameter pattern allowances were all above 2·4%, the predictions are too low by at least 1% on average. This disagreement can be attributed to the expansion of and the hindrance by the outer mould. Recall that the outer mould sand is not taken into account in the simulations, except for the sand between the two cylinders.

In order to estimate the magnitude of the mould expansion and hindrance effects, the following procedure was adopted. Figure 13 shows the predicted displacements of two points (S22 and S7) on the outside diameter in case 1. Point S22 is located on the side of the casting facing the second cylinder, whereas point S7 is located on the opposite side of the cylinder. Because the sand between the two cylinders is included in the simulations, the displacements predicted for point S22 include the effects of (reversible) mould expansion and hindrance, while the displacements for S7 do not. Before solidification, point S22 shows a maximum inward displacement of 0·04 mm (at ~60 s) due to early mould expansion. Since in reality this expansion is irreversible, the 0·04 mm can be added to the predicted contraction at this point. The same amount can be added to the predicted contraction at point S7. In addition, Fig. 13 shows that point S7 undergoes a large outward displacement (expansion) of 0·29 mm before solidification. This can be attributed to the fact that point S7 moves freely (no mould hindrance) in the simulations, and the 0·29 mm outward displacement simply reflects the early expansion of the core pushing on the outer diameter of the casting. Hence, 0·29 mm is added to the predicted contraction at point S7, since in reality the mould would provide sufficient hindrance to prevent the outward movement of the outer cylinder surface before solidification. No such hindrance correction is needed for point S22. A summary of all corrections made for the outer diameter pattern allowances in all four cases is provided in Table 5. The corrected pattern allowances for the outer diameter are in better agreement with the measurements than the pattern allowances predicted directly by the simulations, although they are still somewhat lower. Nonetheless, these rough estimates indicate that the disagreement between the measurements and predictions is indeed due to the neglect of the outer mould in the simulations. More accurate corrections are not possible due to the complex interplay of the various phenomena present.

Conclusions

Experimental data are presented of pattern allowances for cylindrical steel castings. The experiments investigate in detail the effects of the type of sand and binder and of the size of the core. Sand expansion, as well as hindrance of the steel contraction by the sand, was found to play a significant role in determining the final dimensions of the castings. The experimental data are then compared to the results of casting simulations. In several cases the measured and predicted pattern allowance values agree well, instilling some confidence in the simulations. However, there are two shortcomings in the present stress simulations that limit their ability to predict pattern allowances. One is that the irreversible nature of the expansion of silica sand is not taken into account in the simulation. This is particularly important for small cores or other mould portions made with silica sand that reach temperatures higher than ~1200°C (above the quartz to cristobalite phase transformation

Table 5 Effects of outer mould expansion and hindrance on predicted pattern allowances (PAs) for outer cylinder diameter (OD), compared to measured values

	Shrinkage predicted before consideration of expansion of mould sand		Predicted contribution of expansion of mould sand		Shrinkage predicted with correction for expansion of mould sand		Range of measured values
Case	Shrinkage, mm	PA–OD, %	Shrinkage, mm	PA–OD, %	Shrinkage, mm	PA–OD, %	PA–OD, %
1	1·79	1·79	0·37	0·37	2·16	2·16	2·4 to 2·6
2	1·54	1·54	0·43	0·43	1·97	1·97	2·3
3	1·97	1·98	0·48	0·48	2·45	2·45	3·2 to 3·8
4	2·17	2·18	0·20	0·20	2·37	2·37	3·2 to 3·5

temperature). The second shortcoming is that the stress model does not account for the formation of an air gap between the casting and the mould. For that reason, the outer mould typically needs to be excluded from the stress simulations altogether, as was done here. This can cause problems in dimensional predictions when (i) there is significant early sand expansion due to heating of the mould before a solid steel shell forms, and (ii) the solidifying casting does not contract away from the mould but, instead, pushes against the mould resulting in some stress build-up and hindrance to metal contraction. An attempt is made to estimate the magnitude of some of these effects and correct the pattern allowances predicted by the simulation code. It is recommended that the simulation software used in this study be improved to account for the possibility of irreversible sand expansion and air gap formation between the mould and the casting. Overall, the present study provides an improved understanding of the complex physical phenomena that are responsible for dimensional changes in sand casting of steel, and should lead to increased research efforts in this important area.

Acknowledgements

This study was undertaken as part of research funded by the US Department of Energy – Office of Industrial Technologies and the US Department of Defense through the American Metalcasting Consortium (AMC) PRO-ACT programme. AMC's PRO-ACT programme is sponsored by Defense Supply Center Philadelphia (DSC, Philadelphia, PA, USA) and the Defense Logistics Agency (DLA, Ft. Belvoir, VA, USA). This research was conducted under the auspices of the Steel Founders' Society of America, and through substantial in-kind support, guidance and interest from SFSA member foundries. The authors would like to thank MAGMA GmbH for making available the simulation software. Any opinions, findings, conclusions, or recommendations expressed herein are those of the authors and do not necessarily reflect the views of DOE, DSC, DLA, SFSA or any of its member foundries.

References

1. C. A. Sanders: 'Foundry sand practice', 6th edn; 1973, Skokie, IL, American Colloid Co.
2. C. Henschel, R. W. Heine and J. S. Schmucher: *AFS Trans.*, 1966, **74**, 357–364.
3. R. B. Sosman: 'The phases of silica'; 1965, New Brunswick, NJ, Rutgers University Press.
4. J. Campbell: 'Castings'; 1991, Oxford, Butterworth-Heinemann.
5. S. C. Carniglia: 'Handbook of industrial refractories technology'; 1992, Park Ridge, NJ, Noyes Publications.
6. J. B. Andrews, R. N. Andrews and D. Swain: SFSA Research Report 102A, Des Plaines, IL, USA, Steel Founders' Society of America, 1990.
7. W. L. DeKeyser and R. Cypers: *Bull. Soc. Franc. Ceram.*, 1957, **36**, 29–46.
8. C. Bates and J. F. Wallace: *Modern Casting*, May 1966, **49**, 216–227.
9. S. Engler, D. Boenisch and B. Kohler: *Cast Met. Res. J. AFS*, 1973, **9**, 20–30.
10. P. J. Rickards: *Brit. Foundryman*, 1982, **75**, 213–223.
11. E. Ward: *Foundry Trade J.*, 1966, **120**, 601–604.
12. Institute of British Foundry Technical Subcommittee TS71: *Brit. Foundryman*, 1969, **62**, Part 5.
13. Institute of British Foundry Technical Subcommittee TS71: *Brit. Foundryman*, 1971, **64**, Part 10.
14. L. S. Aubrey, T. E. Roberts and P. F. Wieser: SFSA Research Report 84, Rocky River, OH, USA, Steel Founders' Society of America, 1977.
15. T. D. Law: Proceedings of the SCRATA 22nd Annual Conference on 'Steel castings production', Birmingham, UK, 5–6 May 1977, Paper 13.
16. C. W. Briggs and R. A. Gezelius: *AFS Trans.*, 1934, **42**, 449–476.
17. W. H. Moore: *Cast. Eng.*, 1979, **11**, 14–21.
18. J. Kron, M. Bellet, A. Ludwig, B. Pustal, J. Wendt and H. Fredriksson: *Int. J. Cast Met. Res.,* 2004, **17**, 295–310.
19. MAGMASOFT User Manual v4·2; 2003, Aachen, Germany, Magma GmbH.
20. J. Miettinen: *Metall. Trans. B*, 1997, **28B**, 281–297.
21. J. Miettinen and S. Louhenkilpi: *Metall. Trans. B*, 1994, **25B**, 909–916.
22. J. B. Andrews: Private communication and facsimile transmission, January 1996.
23. F. E. Peters: 'Pattern allowance prediction for steel castings', PhD thesis, Penn State University, University Park, PA, USA, 1996.